Mechanism and Performance of SBS Polymer Dry-Modified Asphalt Mixture with PCB and TPO from Waste Tires

Li, Yuanyuan; Li, Jun; Bai, Tao; Chen, Anqi; Gu, Dengjun; Gao, Yangming

DOI
10.1061/JMCEE7.MTENG-16018

Publication date
2024

Document Version
Final published version

Published in
Journal of Materials in Civil Engineering

Citation (APA)
Li, Y., Li, J., Bai, T., Chen, A., Gu, D., & Gao, Y. (2024). Mechanism and Performance of SBS Polymer Dry-Modified Asphalt Mixture with PCB and TPO from Waste Tires. *Journal of Materials in Civil Engineering*, *36*(6), Article 04024099. https://doi.org/10.1061/JMCEE7.MTENG-16018

ASCE

Mechanism and Performance of SBS Polymer Dry-Modified Asphalt Mixture with PCB and TPO from Waste Tires

Yuanyuan Li, Ph.D.[1]; Jun Li[2]; Tao Bai[3]; Anqi Chen[4]; Dengjun Gu[5]; and Yangming Gao[6]

Abstract: Based on the efficient resource utilization of scrap tires, pyrolysis carbon black (PCB), and pyrolysis oil of waste tire (TPO), scrap tires' products were treated using dry styrene-butadiene-styrene (SBS) polymer modification of asphalt. The products of scrap tires, PCB and TPO, were handled using dry SBS polymer modification of asphalt based on the effective resource use of scrap tires. The consequences of scrap tires, PCB and TPO, were taken using dry SBS polymer modification of asphalt based on the effective resource use of scrap tires. PCB and TPO composite effect seriously degraded. Based on this, the impact of dry SBS polymer modification on the functionality of PCB-TPO-modified asphalt and the mechanism of modification was examined. According to the investigation, the SBS polymer was evenly distributed and fully developed in the asphalt mixture, which significantly enhanced the qualities of asphalt and the asphalt mixture and performed a positive role in the internal structure of the asphalt mixture. **DOI: 10.1061/JMCEE7.MTENG-16018.**

Author keywords: Styrene-butadiene-styrene (SBS) polymer; Pyrolytic carbon black; Pyrolytic oil; Modified asphalt; Dry modification.

Introduction

To solve resource shortages and environmental pollution, in addition to vigorously developing green energy, the recycling of solid waste and clean production with low-energy consumption have become increasingly important (Liu et al. 2018). Cui et al. (2021) and Guo et al. (2018) conducted relevant research on the recycling of solid waste, and Wang et al. (2021) conducted in-depth analysis on the life cycle of road energy consumption and relevant sustainable policies. If the recycling of solid waste can be combined with clean production with low-energy consumption (Lee and Kim 2022), it will have a positive significance in reducing energy consumption and environmental protection.

[1]Associate Professor, School of Civil Engineering and Architecture, Wuhan Institute of Technology, Wuhan 430074, China. Email: Liyy@wit.edu.cn

[2]Master's Candidate, School of Civil Engineering and Architecture, Wuhan Institute of Technology, Wuhan 430074, China. Email: 22104010113@stu.wit.edu.cn

[3]Professor, School of Civil Engineering and Architecture, Wuhan Institute of Technology, Wuhan 430074, China (corresponding author). Email: baigs08@wit.edu.cn

[4]Professor, State Key Laboratory of Silicate Materials for Architectures, Wuhan Univ. of Technology, Wuhan, Hubei 430070, China. Email: anqi.chen@whut.edu.cn

[5]Master's Candidate, School of Civil Engineering and Architecture, Wuhan Institute of Technology, Wuhan 430074, China. Email: 22004010016@stu.wit.edu.cn

[6]Professor, Marie S. Curie Research Fellow Section of Pavement Engineering, Faculty of Civil Engineering and Geosciences, Delft Univ. of Technology, Stevinweg 1, Delft, CN 2628, Netherlands. ORCID: https://orcid.org/0000-0001-7310-1476. Email: Y.Gao-3@tudelft.nl

Note. This manuscript was submitted on November 19, 2022; approved on June 6, 2023; published online on March 18, 2024. Discussion period open until August 18, 2024; separate discussions must be submitted for individual papers. This paper is part of the ***Journal of Materials in Civil Engineering***, © ASCE, ISSN 0899-1561.

The safety of the ecological environment is substantially jeopardized and human health is negatively impacted by improper tire disposal (Xu et al. 2021). Therefore, how to dispose of waste tires safely and efficiently is an urgent problem. The most direct treatment method for waste tires is incineration and landfill. However, incineration and landfill seriously pollute the environment and endanger human health (Parthasarathy et al. 2016; Przydatek et al. 2022). Standard tire disposal methods include pyrolysis and grinding used tires into rubber powder (Zhang et al. 2009). Pyrolysis is known as one of the best methods for treating waste tires at present (Sugatri et al. 2018). Compared with the simple physical shearing and grinding process of rubber powder production, it has high resource utilization efficiency, no secondary pollution, and multiple resource recovery and utilization. It can achieve almost 100% environmentally sound treatment (La Rosa et al. 2019). The pyrolysis product of waste tires consists of 35% carbon black (PCB), 45% pyrolysis oil of waste tire (TPO), 10% steel wire, and 10% combustible gas (Min and Jeong 2013). PCB is different from steel wire and combustible gas in the pyrolysis products with wide use and high recovery value. To make industrial goods like activated carbon, paint, and ink, pyrolytic tire carbon black cannot be employed because its performance is not up to par with that of industrial carbon black (Casado-Barrasa et al. 2019).

Aliotti (1962) first proposed that PCB should be used in modified asphalt and determined that the advantages of PCB as an additive were mainly reflected in high-temperature performance. Later research revealed that carbon black can remove light oil components from asphalt and increase the modified asphalt's toughness. As a result, the antirutting and antifatigue properties of the asphalt mixture were enhanced (Konell 2002; Park and Lovell 1996). According to Geckil et al. (2018), modified asphalt containing carbon black can increase the asphalt mixture's durability by reducing the ultraviolet (UV) aging effect. Wang et al. (2022) found that PCB can act as conductive particles to help the asphalt mixture repair internal microcracks in the form of microwave heating.

Feng et al. (2021) found that PCB within 3% has little effect on the performance of asphalt. It was found that the light component in TPO is important for the composite-modified asphalt built of TPO and PCB, which can somewhat improve low-temperature performance but damage asphalt's high-temperature performance (Chen et al. 2022). The large temperature productivity of PCB-modified asphalt can be compromised to achieve a neutral condition and decrease the detrimental effects of PCB on the low-temperature performance of asphalt. However, the preceding studies are all the research results of wet-modified asphalt. In the process of research, it is also found that PCB wet-modified asphalt has problems that are difficult to solve. PCB is insoluble in asphalt and most organic solvents. Although in situ pyrolytic decomposition technology, such as the Wright process, can solve the problem of PCB separation and agglomeration, due to the high cost, it is difficult to achieve large-scale application in wet-modified asphalt pavement. Therefore, wet PCB-modified asphalt's low storage stability and ease of segregation after preparation result in unstable performance of the asphalt mixture and restrict the growth of wet PCB-modified asphalt (Lu et al. 2020b).

Wet-modified bitumen is not a continuous process: the quality of modified bitumen is often reduced during transport and storage, and it tends to segregate when mixed with aggregates, thus reducing the performance of the modified bitumen mix (Lu et al. 2020a). In addition, the wet-modified asphalt also needs to be sheared and swelled for a long time under the temperature of 150°C–200°C. It must use a lot of fuel to maintain the high-temperature environment. This puts a lot of pressure on the environment because it uses a lot of energy and produces a lot of greenhouse emissions (Luo et al. 2022a). Although the process of pyrolysis of carbon black also requires a certain amount of energy consumption, as an asphalt modifier, the proportion of carbon black in the quality of asphalt mixture is very low, and the energy required in the pyrolysis process is far less than the energy consumed in the preparation process of modified asphalt. The preparation of dry-modified asphalt is to directly add the modifier and aggregate into the mixing plant to mix with the asphalt, which directly avoids the problem of segregation of the modified asphalt and ensures the performance stability of the asphalt mixture (Duarte and Faxina 2021). It also reduces the process of transportation, storage, reheating, and mixing of wet-modified asphalt, which not only saves transportation and storage costs and reduces energy consumption, but also avoids the aging problem caused by repeated heating of asphalt (Liu et al. 2021). After styrene and butadiene are polymerized, a copolymer known as styrene-butadiene-styrene (SBS) is created. Styrene gives SBS-modified asphalt its high-temperature strength and tensile qualities, and butadiene gives it its high elasticity, low-temperature flexibility, and fatigue resistance (Yang et al. 2022). It is the most widely used asphalt modification and performs quite well (Lastra-Gonzalez et al. 2022).

This study proposes a method of treating the pyrolysis products PCB and TPO of waste tires using asphalt dry SBS-modified asphalt. In this study, SBS was ground to 0.6 mm to reduce the swelling development time required for SBS, and the transportation process of dry-modified asphalt mixture was simulated. The modified asphalt mixture was placed at a temperature of 170°C for 45 min (Negulescu et al. 2006). The distribution uniformity and dry modification mechanism of PCB- and SBS-modified asphalt were studied using infrared spectroscopy and fluorescence microscopy. Recycling and reusing PCB and TPO using SBS dry modification will provide a new method for recycling waste tires, and bring enormous technical and economic benefits to asphalt materials.

Materials and Experimental Methods

Materials

Asphalt Binder

The test was done in conformity with the test regulations in JTE E20-2011 (MOT 2011). Table 1 lists the primary performance indexes.

Aggregates and Fillers

The particle size of coarse aggregate ranged from 2.36 to 26.5 mm, while the particle size of fine aggregates ranged from 0 to 2.36 mm. Limestone was used as both the coarse and fine aggregates in the totals. Limestone powder that has been finely pulverized served as the filler. Tables 2–4 display the technical indexes. The fill (mineral powder) and aggregate used must match the norms of the JTG E42 technical indices (MOT 2005).

SBS Modifier

The SBS used was produced by Baling Petrochemical, and its technical indexes are provided in Table 5.

PCB and TPO

PCB is the pyrolytic carbon black of waste tires, which is a black powdery solid, and its technical indexes are given in Table 6. TPO is the pyrolysis oil of waste tires, which is a reddish brown liquid, and its technical indexes are given in Table 7.

Table 1. Basic performance indexes of asphalt

Index	Test result	Specification requirement	Test method
25°C penetration (dmm)	71.2	60–80	T0604
Ring & Ball softening point (°C)	48.2	≥46	T0606
10°C ductility (cm)	43.5	≥20	T0605

Table 2. Technical indexes of fine aggregate

Testing parameter	Testing result	Specification requirement	Test method
Apparent relative density	2.782	≥2.5	T0328
Angularity (s)	40.3	≥30	T0345
Sand equivalent (%)	75.2	≥60	T0334

Table 3. Technical indexes of coarse aggregate

Testing parameter	Testing result	Specification requirement	Test method
Apparent relative density	2.785	≥2.5	T0605
Water absorption (%)	0.5	≤2.0	T0308
Crushing value (%)	22.2	≤28	T0316

Table 4. Technical indexes of mineral powder

Testing parameter	Testing result	Specification requirement	Test method
Apparent density (g/cm^3)	2.596	≥2.5	T0352
Plasticity index	3.5	<4	T0351
Hydrophilic coefficient	0.88	<1	T0353

Table 5. SBS technical indexes

S/B	Relative density	Particle size (mm)	Appearance	Tensile strength (MPa)	MFR (g/10 min 200°C, 5 kg)
4/6	0.94	0–0.6	White solid	15	0.1

Table 6. Technical indexes of PCB

Testing parameter	Testing result	Specification requirement	Test method
Ash content (%)	15.3	≦18.5	GB-T 508-85
Water content (%)	1.3	≦2.0	GB 260-77
pH value	6.54	≥6.0	—
Appearance	Black powder	—	—

Table 7. Technical indexes of TPO

Testing parameter	Testing result	Test method
Density (15°C, kg/L)	0.85	GB-T 1884-92
Ash content (%)	0.22	GB-T 508-85
Appearance	Reddish brown liquid	—

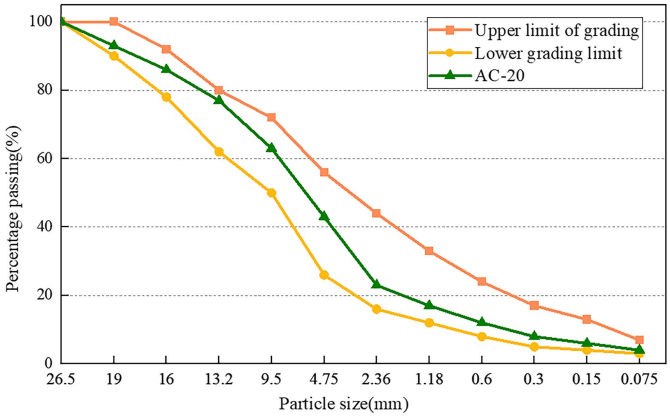

Fig. 1. Grading curve of AC-20 asphalt mixture.

Preparation of Asphalt Mixtures

Gradation Curve of Asphalt Mixture

Fig. 1 shows the selected mixture and its ore gradation curve as an AC-20 densely mixed asphalt mixture with a maximum nominal particle size of 26.5 mm.

Preparation Process of Asphalt Mixture

The original asphalt was chosen to be 70# base asphalt, and the modifiers used were PCB, TPO, and SBS. Table 8 displays the PCB, TPO, and SBS dosages.

There was no pretreatment before the PCB and TPO test, but the SBS needed to be pulverized to less than 0.6 mm. The purpose of pulverization was to accelerate the swelling process of SBS in the asphalt mixture to achieve the purpose of dry modification. In the actual project, the asphalt mixture is mixed in the mixing building and spread on the construction site, which takes a certain amount of time. As a result, the blended modified asphalt mixture was baked at 170°C throughout the test.

Following the preparation of each batch of asphalt mixes, the high-temperature stability was evaluated using a rutting test, and the low-temperature fracture resistance was evaluated using a semicircle bending test (SCB); the water stability was tested by freeze–thaw split test and water immersion Marshall test; and the fatigue property was tested by semicircular bending test (cyclic semicircle bending tensile test (R-SCB)]. The test flowchart is shown in Fig. 2.

Volume Parameters

The asphalt mixture utilized has a gradation of AC-20, a design porosity of 4%–6%, and an asphalt aggregate ratio of 4.2%. Table 9 displays the volumetric characteristics of the asphalt mixture.

Experimental Methods

Asphalt Component Change Test

Fourier transform infrared spectroscopy attenuated total reflectance (FTIR-ATR) was used to measure the wavelength absorption difference of different substances in asphalt to measure the changes of four asphalt functional groups and chemical bonds.

Micromorphology Test of PCB

After the PCB was vacuum prepared, the morphology of the PCB micro samples was examined using scanning electron microscopy (SEM) pictures taken with a Hitachi (Tokyo) Regulus 8100 scanning electron microscope.

Physical Properties of Asphalt

The SBS-modified asphalt was sheared at 170°C for 45 min with a high-speed shear apparatus at a rotating speed of 3,000 rpm, and then was poured into the molds of penetration, softening point, and ductility. After waiting for the corresponding time, the surfaces of the test specimens were scraped flat and placed in the penetrometer, softening point tester, and ductility machine. The corresponding performances were tested after holding at the corresponding temperature for a certain time.

Rheological Properties of Asphalt

A dynamic shear rheometer (DSR) was employed to examine the rheological characteristics of asphalt. The test temperature was

Table 8. Components and proportions of asphalt mixture mix proportion

Asphalt mixture type	Abbreviation	Type and content of dosage mixture modifier		
		PCB (%)	TPO (%)	SBS (%)
70# asphalt	70#	—	—	—
70# + 16% PCB	70# + P	16	—	—
70# + 16% PCB + 1% TPO	70# + P + T	16	1	—
70# + 16% PCB + 1% TPO + 4%SBS	70# + P + T + S	16	1	4

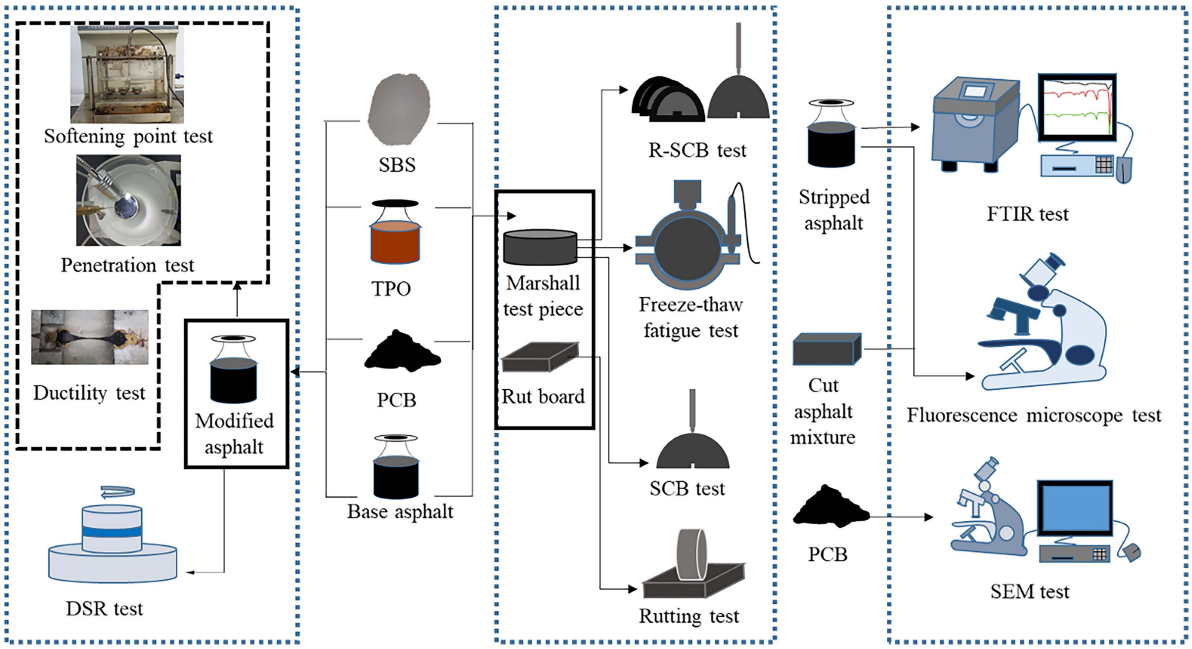

Fig. 2. Asphalt mixture test process.

Table 9. Volume parameters of asphalt mixture

Mixture type	Void ratio (%)	Mineral aggregate void ratio (%)	Asphalt saturation (%)
70#	5.8	14.3	59.4
70# + P	5.4	16.0	66.19
70# + P + T	4.3	14.0	69.3
70# + P + T + S	4.5	14.6	69.2

adjusted between 51.45°C and 87.23°C, and the scanning temperatures were set by strain at quite a frequency of 10 rad/s.

Fluorescence Microscope

Suitable asphalt-coated particles were selected and then photographed in a dark room using a blue light source. The pump light was corrected so the light source was properly focused and the field of view was enhanced, and then the images were captured and processed.

Marshall Stability Test

The classic Marshall test piece was soaked in a 60°C water bath for half an hour before testing.

Rutting Test

The rut board was put into the rut tester and kept at 60°C for 5 h, then the test was started and the test data were automatically generated by the rutting tester.

Low-Temperature Performance Test

The Marshall semicircle sample was put into the UTM-100 constant temperature box (Sydney, Australia), placed at −10°C for 4 h, and then the UTM-100 was used for the SCB test.

Water Loss Resistance

The water loss resistance of the asphalt mixture can be evaluated with the help of the water immersion Marshall test as well as the freeze–thaw split test.

Fatigue Performance Test

The fatigue performance of asphalt mixture was evaluated by cyclic semicircle bending tensile test (R-SCB). UTM-100 was used to measure the bending tensile strength of the semicircle, while the other semicircle was used to test the loading time at a certain stress ratio until the specimen was damaged. The design stress ratios were 0.7, 0.6, 0.5, 0.4, and 0.3.

Results and Discussion

Modification Mechanism of Dry SBS-Modified Asphalt

Surface Micro Morphology

Fig. 3 is the SEM images of different multiples of PCB, which are 2,000×, 5,000×, 7,000×, and 10,000×, respectively. It can be seen from the images of 2,000× and 5,000× that PCB is a spherical block formed by mutual attraction under the action of intermolecular force, and the particle size range of PCB is about 1–6 μm. It can be observed from the 2,000× SEM image that PCB can further agglomerate into irregular agglomerates. Large-area agglomeration was not observed under 5,000× magnification, and there was a clear boundary between aggregates when the particle size exceeds 6 μm, which indicated that the connection between aggregates with particle size beyond a certain range is weak, which was conducive to the uniform dispersion of PCB in asphalt mixture. It can be seen from the observation of 7,000× and 10,000× SEM scales that there were a large number of nanoscale heterogeneous carbonaceous sediments (Li et al. 2022a) distributed on the surface of PCB particles that accumulate and form irregular coral-like substances. During the stretching and tearing process of wet-modified asphalt, the location of PCB is called the stress concentration point. PCB with more carbonaceous deposits and poor interlayer bonding with asphalt were easy to break (Kumar et al. 2022), which made wet PCB-modified asphalt prone to segregation and had a certain impact on the preparation of wet-modified asphalt and the storage stability during transportation (Korayem et al. 2020). However,

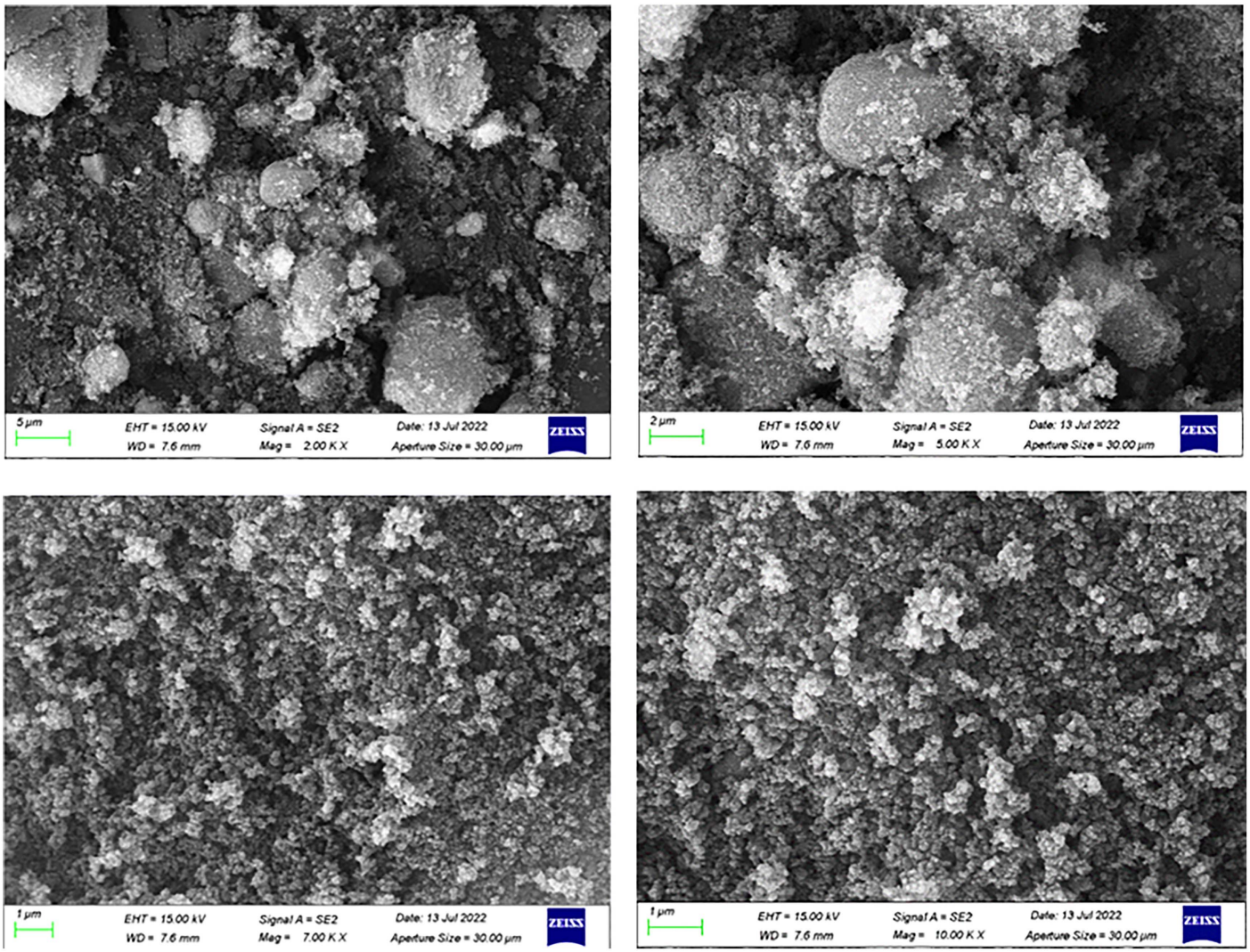

Fig. 3. Microstructure of carbon black.

the preparation of dry PCB-modified asphalt mixture did not involve the preparation and transportation; therefore, the performance of PCB-modified asphalt mixture constructed by dry method was more stable.

Chemical Structure of Dry SBS-Modified Asphalt

When irradiating molecules with infrared light, the absorption frequencies of different chemical bonds or functional groups in the molecules are different, and the absorption peaks at different locations will be displayed on the infrared spectrum, and the information of different chemical bonds or functional groups in the molecules can be obtained (Li et al. 2021b). Infrared spectrometer tests were conducted on samples of the asphalt in the four groups of asphalt mixes stripped with trichloroethylene to see how the chemical bonds and functional groups had changed. The test results are displayed in Fig. 4. The infrared spectrum study reveals that the asphalt infrared spectrum in each of the four types of asphalt mixtures appears in the exact location, and the main wave peaks appear near 2,921, 2,825, 1,428, and 874 cm^{-1}. According to the infrared absorption spectrogram, the analysis results are as follows: 2,921 cm^{-1} is the asymmetric stretching vibration peak of -CH_2; 2,825 cm^{-1} is the symmetric stretching vibration peak of -CH_2; 1,428 cm^{-1} is the bending vibration peak in saturated C-H plane; and 874 cm^{-1} is the flexural vibration peak in the olefin unsaturated C-H plane (Li et al. 2021a), which indicates that the chemical composition of asphalt in the four asphalt mixtures has certain similarity. PCB, TPO, and SBS are physically blended after being mixed with asphalt, and no chemical reaction occurs to form new chemical bonds.

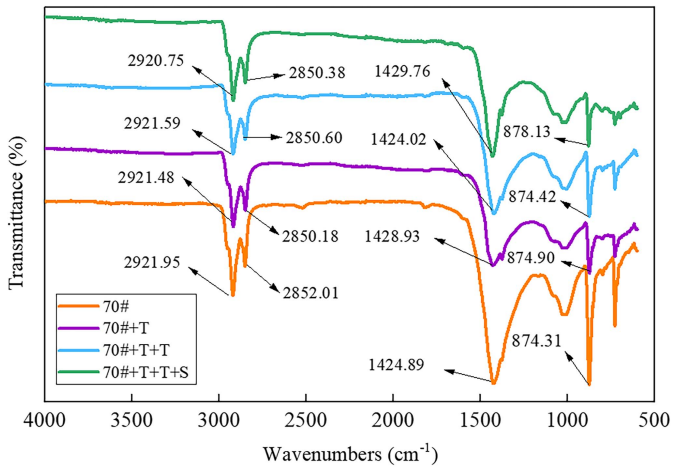

Fig. 4. Test results of infrared spectrum of asphalt.

J. Mater. Civ. Eng., 2024, 36(6): 04024099

The modifiers in the four modified asphalts did not react with the asphalt to form new chemical bonds; however, the content of each component of the modified asphalt may change. To determine the change in the ratio of the area of the characteristic peak to the total size of the characteristic peak, which is used to characterize the difference in the proportion of asphalt components, the place and height of the distinct peaks of the four modified asphalts at 1,428 and 874 cm^{-1} were calculated using OMNIC software. The location of the two characteristic peaks was compared with the entire region of the distinct peaks at 500 to 2,000 cm^{-1} (Luo et al. 2022b). The calculation results are given in Table 10. It can be seen from the chromatogram that 1,424 and 874 cm^{-1} correspond to alkanes and aromatics, respectively. The area proportion of the characteristic peak at 1,424 cm^{-1} of asphalt added with PCB decreases by 7.4%, and the peak height decreases by 0.173. Although the addition of PCB may block infrared radiation and affect the height of its peaks, in this study the latter 70# + T, 70# + P + T, and 70# + P + T + S all contain the same amount of carbon black, but the changes in the peaks of 70# and 70# + T are not significant, so the peak height changes caused by carbon black may not be the main reason. The most obvious change in peak height is the addition of TPO. This shows that after PCB is added, it absorbs some alkanes in asphalt, that is, light components of asphalt, thus reducing the concentration of alkanes in asphalt. The area ratio and height of the characteristic peak at 874 cm^{-1} decreased, indicating that PCB also absorbed some olefins. After adding TPO to 70# + P, the area of the characteristic peak of the infrared spectrum of 70# + P + T-modified asphalt increased by 14.1%, and the height of the characteristic peak increased by 0.173. This indicates that the addition of TPO increases the lightweight components of the modified asphalt and absorbs more lightweight components than carbon black. The area ratio and height of the characteristic peak did not change much, indicating that there may be only a small amount of olefins in the TPO. After adding SBS to 70# + P + T, the proportion and height of the characteristic peak area at 1,424 cm^{-1} decreased by 3.4% and 0.087, respectively, and SBS absorbed the light components in the asphalt and only a minor percentage of the olefins throughout the swelling process, as shown by the proportion and height of the typical peak region at 874 cm^{-1}.

The performances of asphalt and asphalt components have a strong correlation; after the PCB is added to the asphalt absorbed part of the lighter components of asphalt resulting in a relative reduction in its content, the asphalt content of asphalt will be relatively increased, which may lead to an increase in the needle penetration of asphalt, as shown by the increase in the high-temperature performance of asphalt mixtures, while at the same time may reduce the ductility of asphalt, as shown by the low-temperature asphalt.

Table 10. Height and area ratio of spectral characteristic peak of modified asphalt

Location of characteristic peak (cm^{-1})	Type of modified asphalt	Proportion of characteristic peak area (%)	Height
1,424	70#	42.57	0.402
	70# + P	35.22	0.229
	70# + P + T	49.36	0.402
	70# + P + T + S	45.98	0.315
874	70#	6.07	0.312
	70# + P	4.96	0.189
	70# + P + T	4.89	0.216
	70# + P + T + S	4.21	0.195

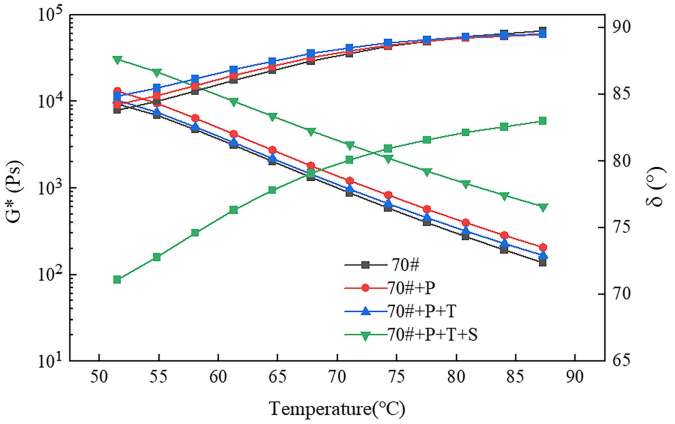

Fig. 5. Shear composite modulus (G^*) and phase angle.

The low-temperature performance of asphalt may be reduced (Sun et al. 2020). The addition of TPO to asphalt supplements the lighter components reduced by the addition of PCB, thus reducing the high-temperature performance of the asphalt mixture and improving the low-temperature performance of the asphalt mixture. The ratio of PCB to TPO in this study makes the high- and low-temperature performance of asphalt tend to be similar to that of the as-built asphalt.

Physical and Rheological Properties of Composite-Modified Asphalt

The composite shear modulus and phase angle of the matrix and modified asphalt are shown in Fig. 5. The complex shear modulus (G^*) measures relatively robust asphalt to denting when subjected to repetitive, cyclic shear stress. The greater the value, the more resistant asphalt is to deformation. The asphalt's viscosity to elasticity is represented by the asphalt's phase angle (δ). The smaller the phase angle, the better the elasticity of asphalt. Fig. 6 is the graph of four asphalt rutting factors ($G^*/\sin\delta$). The larger the rutting factor, the better the high-temperature performance of asphalt. The composite shear modulus and rutting factor values of 70# + P are higher than those of 70# base asphalt. The phase angles are almost the same as those of the 70# base asphalt, as shown in Figs. 5 and 6, indicating that the addition of PCB increases the resistance of the asphalt to high-temperature deformation. However, the composite shear modulus, phase angle, and rutting factor curves of

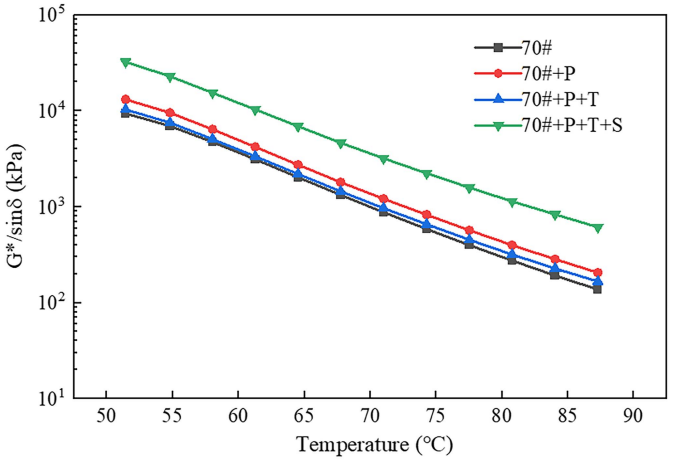

Fig. 6. Rut factor (G = sin δ).

Table 11. Physical property data of composite-modified asphalt

Asphalt type	Penetration (dmm)	Softening point (°C)	Ductility (10°C) (mm)
70#	73.7	47.4	236.3
70# + P	51.6	50.5	101.6
70# + P + T	61.4	44.6	155.7
70# + P + T + S	42.6	74.1	544.5

70# + P + T were very similar after the addition of TPO, indicating that the addition of TPO reduced the high-temperature performance of the asphalt to the high-temperature properties of the original asphalt. The value of composite shear modulus and rutting factor of 70# + P + T + S is the largest and the value of phase angle is the smallest among the four asphalts, which indicates that the addition of SBS can enhance the ability of asphalt to resist repeated shear deformation at high temperature (Table 11). It can be seen from this data analysis that the test results of the three major indicators of asphalt are similar to those of the dynamic shear rheology test of asphalt. Adding PCB will boost asphalt's high-temperature performance, adding TPO will reduce asphalt's high-temperature performance, and adding SBS will greatly enhance asphalt's high-temperature performance.

Fluorescence Analysis of Dry SBS-Modified Asphalt

By exposing SBS-modified asphalt to fluorescence microscopy blue light, fluorescence microscopy can be acquired, and the distribution condition of SBS in asphalt may be assessed (Asib et al. 2022). Fig. 7(a) is a fluorescence image of asphalt peeled from the surface of the mixture using an asphalt extractor, and Fig. 7(b) is a fluorescence image directly irradiated on the surface of the asphalt mixture. When directly sampling from the asphalt mixture, the display image of the fluorescent microscope has a great correlation with the cleanliness of the aggregate and mineral powder in the asphalt mixture because the aggregate and mineral powder may contain a certain amount of fluorescent minerals (Huang et al. 2021), thus affecting the test results. Irregular flaky fluorescent substances can be observed from both Figs. 7(a and b), but they are less distributed in general and have little impact on the test. From the fluorescence microscopy images of Fig. 7(a), it can be distinguished that SBS is mainly distributed in the asphalt mixture as a dispersed phase of dotted gray color and does not form a continuous phase, and it can be observed that the brightness and diameter of the fluorescence images of SBS vary widely, which indicates that the dry SBS-modified asphalt absorbs the lighter components of the asphalt during the process of mechanical mixing and the regeneration process leading to the SBS in the internal volumetric expansion (Jahanbakhsh et al. 2018; Wu et al. 2011). From Fig. 7(b), it can be concluded that SBS is more evenly distributed in the asphalt mixture, there is no significant accumulation, and the dispersion is also distributed as dots within the asphalt mixture. Combined with Figs. 7(a and b) fluorescence microscopic images, it can be analyzed that the SBS in the dry SBS-modified asphalt mixture is dispersed more uniformly in the mechanical mixing process, and the SBS absorbs the lightweight components in the asphalt during the mixing and health maintenance process, resulting in volume expansion, which makes SBS play a role in structural reinforcement in the internal structure of the asphalt mixture, thereby improving the road performance of the asphalt mixture.

Road Performance of Asphalt Mixture

Mechanical Properties

The Marshall stability and Marshall modulus of four distinct asphalt mixtures are shown in Fig. 9. According to Fig. 8, the Marshall stability of 70# + P is 19.5% higher than the 70# asphalt mixture. The Marshall stability of 70# + P + T is 29.9% and 8.7% higher than that of 70# and 70# + P. The Marshall stability of 70# + P + T + S increases by 70.1%, 42.3%, and 31.0%, respectively, compared with that of 70#, 70# + P, and 70# + P + T asphalt mixtures. The ratio of the Marshall stability of the asphalt mixture to the flow value of the asphalt mixture determines the asphalt mixture's Marshall modulus, which gauges the asphalt mixture's ability to resist load in unit deformation. Experimental results is depicted in Fig. 9. The Marshall modulus of 70# + P is larger than the 70# and 70# + P + T asphalt mixtures, and the Marshall modulus of 70# asphalt mixture is almost the same as that of 70# + P + T.

From Fig. 8, it can be seen that after PCB is added to 70# asphalt mixture, both the Marshall stability and the Marshall modulus of 70# + P are increased. This shows that the addition of PCB not only increases the load resistance of asphalt mixture, but also improves the load resistance of asphalt mixture per unit deformation. The reason may be that the addition of PCB absorbs the lightweight components of asphalt at the same time with the mechanical mixing force. The asphalt mixture contains heterogeneous carbonaceous deposits on the surface of PCB particles, which reduces the asphalt's ductility and enhances its mechanical qualities. From Table 9, with the addition of TPO, the voidage of 70# + P + T decreased by 25.6%. This demonstrates that the inclusion of TPO reduces the viscosity of the modified asphalt mixture, increasing its compactness. The Marshall stability of 70# + P + T is slightly

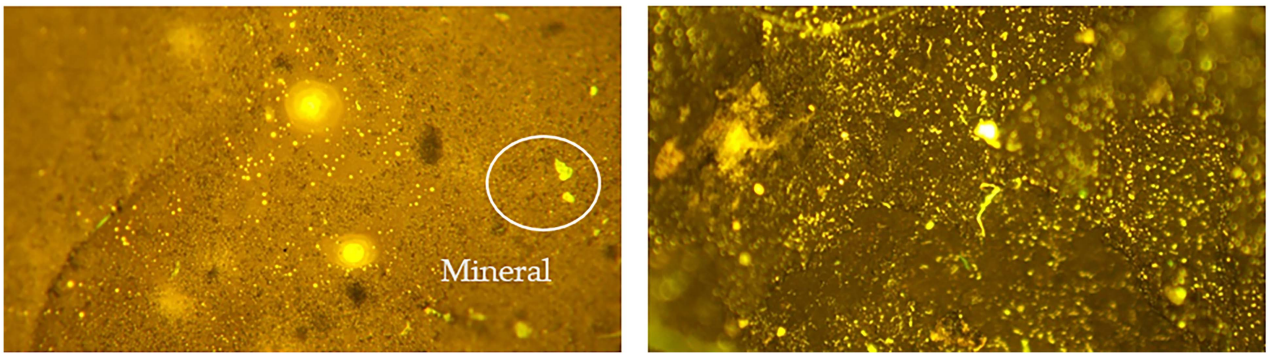

Fig. 7. Fluorescent images of (a) stripped asphalt; and (b) asphalt on aggregate surface.

higher than that of 70# + P, but the Marshall modulus is lower, as can be seen in Figs. 8 and 9. This demonstrates that while the strength of the asphalt mixture somewhat increases with the addition of TPO, the resistance to load per unit deformation reduces.

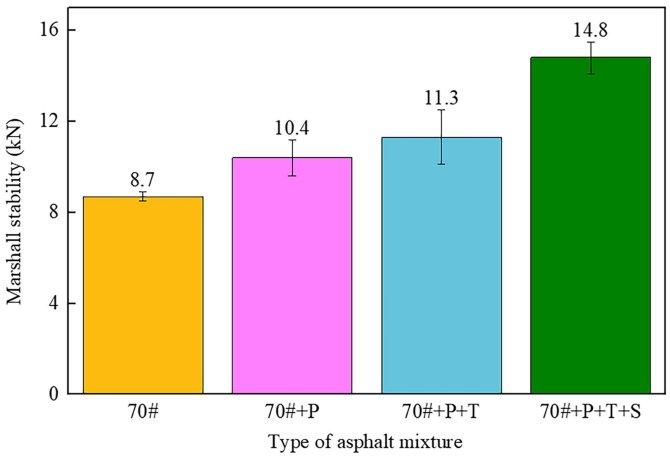

Fig. 8. Marshall stability of asphalt mixtures.

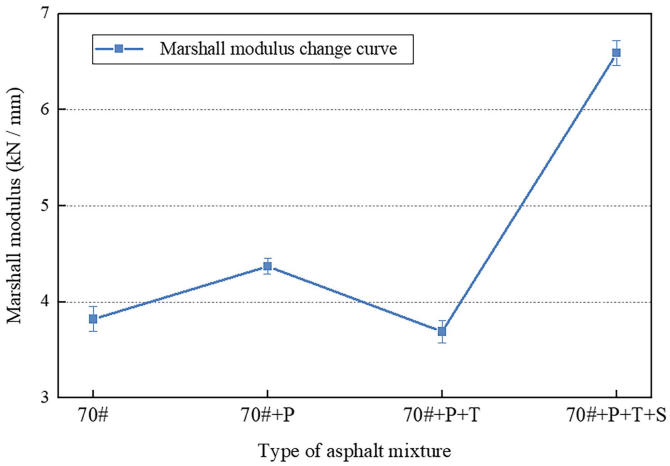

Fig. 9. Marshall modulus of asphalt mixtures.

The reason may be that TPO complements the lightweight components of the asphalt mixture to reduce the viscosity of the asphalt. As a result, the ability to resist load per unit deformation becomes lower, and the reason for the slight increase of Marshall stability of 70# + P + T may be that the decrease of 70# + P + T voidage increases the intercalation force between aggregates in asphalt mixture. As a result, the asphalt mixture's capacity to withstand load is improved, which increases its Marshall stability. The Marshall stability and Marshall modulus significantly increase when SBS is added to the asphalt mixture, indicating that SBS can enhance the mechanical properties of the asphalt mixture.

Rutting Resistance at High Temperature

The rutting test mimics the motion of moving cars over hot asphalt pavement. Rutting depth and dynamic stability assess an asphalt mixture's resistance to rutting at high temperatures (Li et al. 2022b). Fig. 10 displays the findings from tests on the asphalt mixture's resistance to rutting at high temperatures. Fig. 10 shows that compared with 70# asphalt mixture, 70# + P asphalt mixture has 63.7% higher dynamic stability. Rutting depth is less than that of 70# asphalt mixture by 0.170 mm. This demonstrates how PCB enhances the asphalt mixture's resistance to rutting at high temperatures. The dynamic stability of 70# + P + T is 57.2% lower than that of 70# + P, and the rutting depth is deeper 0.357 mm. Its dynamic stability is less than 70# asphalt mixture and the rutting depth is more than 70# asphalt mixture. This demonstrates that including TPO decreases the asphalt mixture's high-temperature rutting resistance. The dynamic stability of 70# + P + T + S is 341.57%, 169.7%, and 530.6% higher than that of 70#, 70# + P, and 70# + P + T asphalt mixtures. The rutting depth of 70# + P + T + S is only 0.099 mm. This demonstrates how adding SBS significantly enhances the asphalt mixture's resistance to rutting at high temperatures.

According to the test results, it is difficult only to use PCB as a modifier to improve the rutting resistance of the asphalt mixture. If we continue to increase the content of PCB, it may continue to improve the high-temperature performance of asphalt mixture, but it is bound to affect other performance. So it is difficult to use PCB dry-modified asphalt in practical engineering. When SBS is added, the high-temperature rutting resistance of asphalt mixture has been greatly improved. Perhaps due to external mechanical forces and intermolecular forces acting on SBS and asphalt. They entwined,

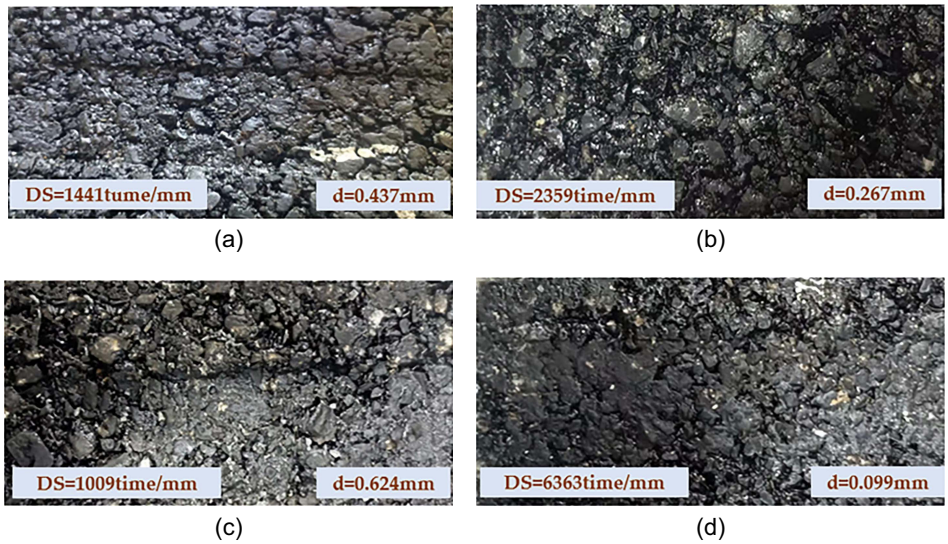

Fig. 10. Rutting test results of asphalt mixture: (a) 70#; (b) 70# + P; (c) 70# + P + T; and (d) 70# + P + T + S.

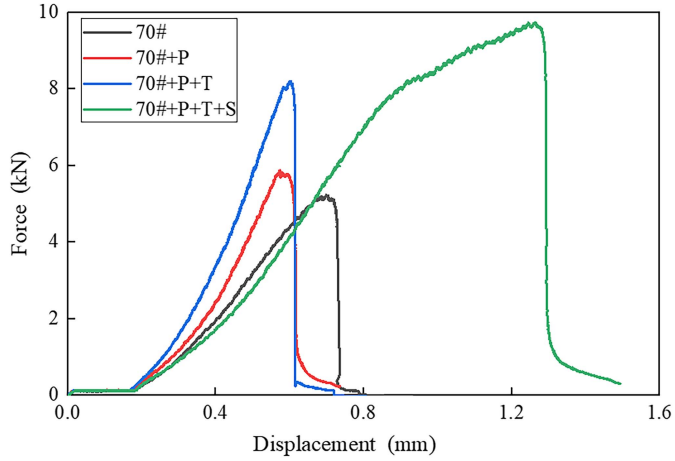

Fig. 11. Fracture curves of asphalt mixtures.

strengthening the asphalt mixture's internal structure and significantly enhancing its resistance to rutting at high temperatures.

Cracking Resistance at Low Temperature

Cracking of asphalt pavement, especially in low-temperature environments, is related to the asphalt mixture's good low-temperature performance (Wu et al. 2022). Therefore, enhancing the asphalt mixture's low-temperature fracture resistance is a crucial component of the actual use of asphalt roads. The test outcomes are displayed in Figs. 11 and 12. The load and displacement curve of the asphalt mixture is shown in Fig. 11, and the fracture energy of the asphalt mixture is shown in Fig. 12. According to Fig. 11, the load and fracture displacement of 70# + P + T + S at low temperature are the largest, and the load and displacement curves of the other three groups of asphalt mixtures are not significantly different, so it can be preliminarily judged that # + 70 P + T + S has the best low-temperature crack resistance and there is little difference in low-temperature performance of the other three groups. As shown in Fig. 12, the fracture energy of the 70# + P asphalt mixture is 4.9% lower than that of the 70# asphalt mixture, suggesting that the addition of PCB has little impact on the asphalt mixture's resistance to low-temperature cracking. The fracture energy of 70# + P + T is 32.5% higher than that of 70# + P, which indicates that the addition of TPO can increase the low-temperature performance of asphalt mixture. In comparison to the 70#, 70# + P, and 70# + P + T asphalt mixtures, 70# + P + T + S has a fracture energy that is 144.1%, 156.8%, and 93.9% higher, respectively. This demonstrates that using SBS improves the asphalt mixture's low-temperature crack resistance.

According to the preceding information, adding PCB decreases the asphalt mixture's ability to resist cracking at low temperatures, whereas adding TPO increases that ability. The reason may be due to the low or high doping ratio of PCB and TPO. As shown in Fig. 12, the fracture energy of the 70# + P asphalt mixture is 4.9% lower than that of the 70# asphalt mixture, suggesting that the addition of PCB has little impact on the asphalt mixture's resistance to low-temperature cracking. If we continue to increase TPO, its high-temperature performance may further decline, so even though TPO can enhance the low-temperature performance of asphalt mixture, the content of TPO cannot be further increased due to other performance limitations. It can be predicted that if the content of PCB continues to be increased, the low-temperature performance of asphalt mixture will further decline. As stated previously, the addition of PCB reduces the asphalt lightweight component, while the addition of TPO increases the asphalt lightweight component. This affects how well asphalt performs in high and low temperatures and how well 70# + P and 70# + P + T perform in low temperatures. After being added to the asphalt mixture, SBS absorbs the expansion of the lightweight components, strengthening the asphalt mixture's internal structure and enhancing its performance at low temperatures.

Resistance to Water Damage

The immersion Marshall test primarily replicates the breakdown of water molecules on the adhesion between aggregate surface and asphalt in asphalt mixture. Additionally, the freeze–thaw splitting test replicates the internal wetness of the asphalt mixture and the volume change brought on by the change in ambient temperature, which results in the inside of the asphalt mixture being damaged. The immersion Marshall test results of four kinds of asphalt mixtures are shown in Fig. 13, and the freeze–thaw splitting test results are shown in Fig. 14. According to Fig. 13, the water immersion residue of four kinds of asphalt mixtures has little difference, which is mainly shown as the lowest water immersion residue of 70# + P and the highest water immersion residue of 70# + P + T. Among them, the water immersion residue of 70# + P + T is more than 100%. The reason may be that the immersion Marshall value of the asphalt mixture itself is close to 100% and the inevitable error in the test. It can be seen from Fig. 14 that the freeze–thaw splitting ratio (TSR) of the 70# + P asphalt mixture is the lowest among the

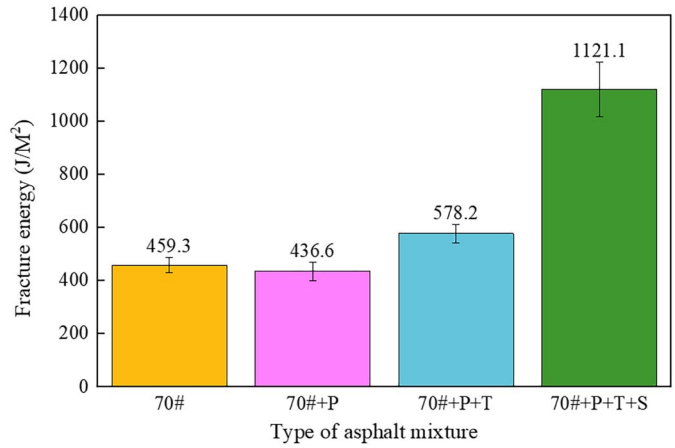

Fig. 12. Fracture energy of asphalt mixture.

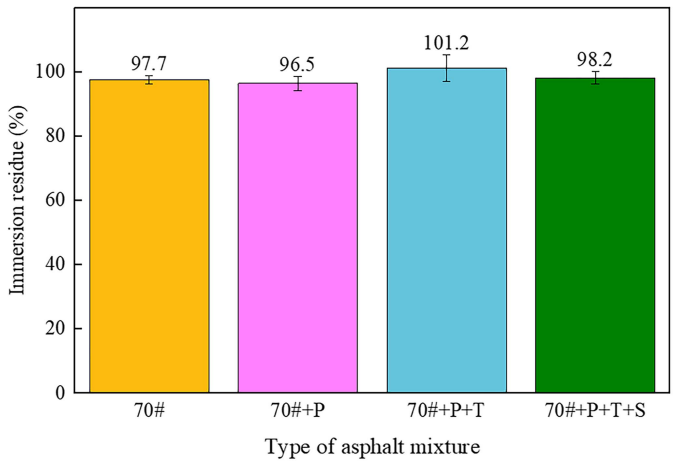

Fig. 13. Immersion Marshall test data.

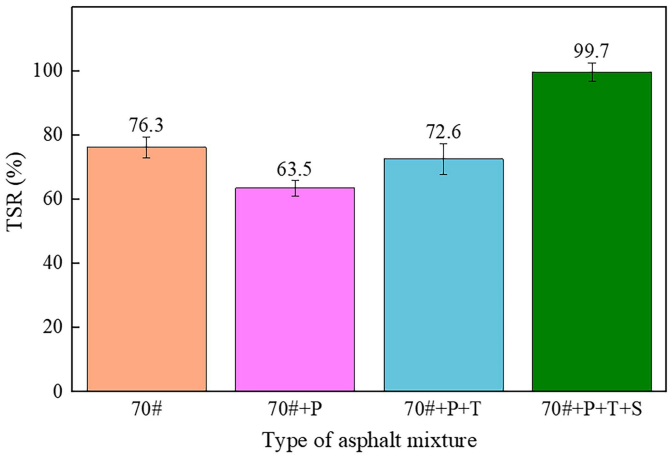

Fig. 14. Freeze–thaw split test data.

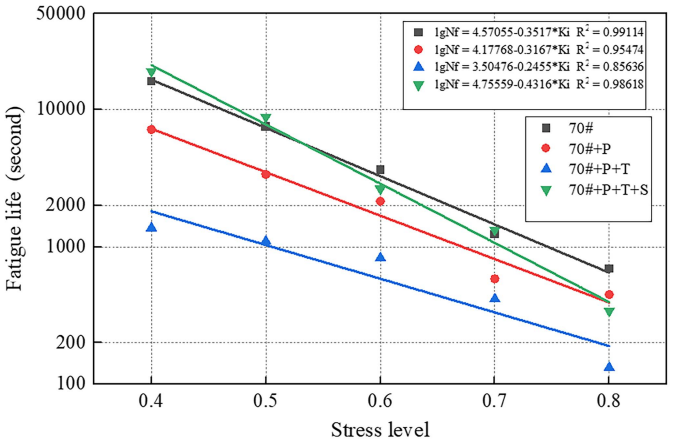

Fig. 15. Fatigue stress and loading times curves of asphalt mixtures.

four asphalt mixtures. The TSR of 70# + P is 16.8% lower than that of the 70# asphalt mixture TSR and 12.5% lower than that of the 70# + P + T TSR. This demonstrates that whereas the addition of TPO increases the internal cohesion of the asphalt mixture, the addition of PCB decreases its internal cohesion. The TSR of 70# + P + T + S is higher than that of the 70#, 70# + P mixture, and 70# + P + T asphalt mixtures by 30%, 57%, and 37.3%, respectively. This demonstrates that the inclusion of SBS can increase the water loss resistance of the asphalt mixture when combined with the test data from the submerged Marshall and freeze–thaw splitting data.

The degree of adhesion between the asphalt and aggregate surface and the cohesiveness of the asphalt mixture are the two key factors influencing how resistant the asphalt mixture is to water loss. The adhesion of asphalt aggregate is not only related to the performance of asphalt itself, but also related to the type, angularity, acidity, and alkalinity of aggregate (Zhang et al. 2021). The same aggregate and gradation were used in this study, so the difference in adhesion between asphalt and aggregate caused by aggregate can be eliminated. The test results show that the addition of PCB and TPO has little effect on the adhesion between asphalt and aggregate, which makes the immersion Marshall residual value of 70# asphalt mixture not different from that of 70# + P and 70# + P + T. Because the viscosity of asphalt is increased by the addition of SBS, this potentially improves the adhesion between 70# + P + T + T asphalt and aggregate. However, the immersion Marshall test findings do not demonstrate this enhancement in asphalt adhesion with the addition of SBS. In addition to the adhesion between the asphalt and the aggregate, the viscosity, porosity, and structural strength of the asphalt mixture all affect how well it adheres inside (Lee 2016). Because PCB was added, the cohesiveness of the asphalt mixture was reduced, and as a result the TSR value of the 70# + P asphalt mixture is lower than that of the 70# asphalt mixture. This lower TSR value decreases the asphalt mixture's resistance to water damage. As mentioned previously, the addition of TPO reduced the void fraction of the asphalt mix, which in turn reduced the effect of water absorption and water molecule volume expansion on the internal structure of the asphalt mix. As a result, the TSR value of 70# + P + T was higher than that of 70# + P and the resistance to water loss of the asphalt mixture was increased. When SBS is added to the asphalt mixture, it not only increases the viscosity of the asphalt in the asphalt mixture, but also enhances the internal structure of the asphalt mixture due to the cross-linking between SBS and asphalt, thus increasing the water loss resistance of the asphalt mixture and therefore the cohesion of the asphalt mixture.

Antifatigue Performance

The fatigue resistance of the asphalt mixture was evaluated by cyclic semicircle bending test. The fitting curve and stress ratio curve of loading times are shown in Fig. 15. According to Fig. 15, the residual values of fatigue fitting curves of four kinds of asphalt mixtures are all greater than 0.85. This demonstrates how closely the four fitting curves are connected to the data values. The fatigue performance of 70# + P + T is the poorest, while the fatigue performance of 70# + P is only slightly better than that of 70# + P + T, as seen from the fatigue curves. This demonstrates that the inclusion of PCB and TPO degrades the fatigue resistance of the asphalt mixture and shortens its fatigue life. It can be seen from the figure that there is little difference in fatigue performance between 70# + P + T + S and 70#. The loading times of 70# + P + T + S at high stress ratio are lower than those of the 70# asphalt mixture, but at low stress ratio the loading times of 70# + P + T + S are higher than those of the 70# asphalt mixture, which shows that the fatigue life of 70# + P + T + S under low load is better than that of the 70# asphalt mixture, but the fatigue life of the 70# asphalt mixture under high load is lower than that of the 70# asphalt mixture. Although the fatigue performance of 70# + P + T + S is not significantly different from that of the 70# asphalt mixture, the addition of SBS can improve the fatigue performance of the asphalt mixture. However, because of the poor fatigue performance of 70# + P + T, the fatigue performance of the asphalt mixture added with SBS can only be restored to the level of the original asphalt mixture. To summarize, the addition of PCB and TPO will reduce the fatigue performance of the asphalt mixture, decrease in degree from fatigue curve. As can be seen, the effect of TPO addition on asphalt mixture fatigue performance is more substantial. SBS can improve an asphalt mixture's fatigue performance, but under the mixture ratio and modifier content used in this study, the asphalt mixture's fatigue performance can only be raised to the level of the original asphalt.

Conclusions

The physical and rheological characteristics of composite-modified asphalt as well as the mechanical characteristics and road performance of asphalt mixture were examined based on the study of micromechanics and performance of asphalt mixture and asphalt binder. The following conclusions can be made:

- Through the SEM diagram, it is found that there is a clear boundary between the PCB agglomerates with a radius of more than

6 μm, which indicates that the connection between the agglomerates whose particle size exceeds a certain range is weak, which is beneficial for PCB to be uniformly dispersed in the asphalt mixture.

- PCB can reduce the content of alkanes and olefins in asphalt, TPO will increase the content of light components in asphalt, and SBS will also absorb the light components in asphalt, indicating that the composition of asphalt can be adjusted by adjusting the ratio of PCB, TPO, and SBS.
- Asphalt's resistance to deformation at high temperatures will increase thanks to PCB, while its performance at low temperatures will decline. TPO can be used to mix asphalt materials to enhance PCB-modified asphalt's low-temperature performance while lowering its high-temperature performance. SBS can be wound with asphalt to improve the structure, enhancing PCB-TPO composite-modified asphalt's high-temperature deformation resistance and low-temperature performance. SBS during the dry SBS process is more evenly distributed in asphalt at the same time as swelling forms.
- The dry modification of PCB can increase the asphalt mixture's high-temperature rutting resistance but decrease its low-temperature cracking resistance and water loss resistance. The low-temperature cracking resistance and water loss resistance of asphalt modified by the PCB dry method supplemented with TPO have recovered to a large extent, but the high-temperature rutting resistance brought by TPO addition also decreased to the near that of the original asphalt. SBS can strengthen the structure of asphalt mixture and greatly improve the high and low temperature, water loss resistance, and fatigue resistance of PCB-TPO dry-modified asphalt mixture, thus meeting the requirements of road pavement.
- The dry modification provides a promising approach for the safe treatment and usage of waste tires, as well as the ability to save asphalt, consume the pyrolysis products of waste tires, improve the performance of modified asphalt materials, conserve resources, and safeguard the environment.

Data Availability Statement

Some or all data, models, or code that support the findings of this study are available from the corresponding author upon reasonable request.

Acknowledgments

The authors acknowledge the Transportation Technology Project of the Department of Transport of Hubei Province (No. 2022-11-1-10), the Scientific Research Fund Project of the Wuhan Institute of Technology (No. K2021032), the Strength Formation Mechanism and Application of Self-Compacting Asphalt Pavement Materials at Ambient Temperature for Urban Roads of the Science and Technology Planning Project of the Hubei Provincial Department of Housing and Urban-Rural Development (No. 202171), European Union's Horizon 2020 Research and Innovation Programme under the Marie Skłodowska-Curie grant agreement (No. 101030767), and the test help from Shiyanjia Lab (Wuhan, Hubei Province, China).

References

Aliotti, A. G. 1962. "Carbon black—Its nature and possible effects on the characteristics of bituminous road binders." In *Proc., 1st Australian Road Research Board (ARRB) Conf.* Melbourne, VIC, Australia: Australian Road Research Board.

Asib, A. M., R. Rahman, P. Romero, M. P. Hoepfner, and A. Mamun. 2022. "Physicochemical characterization of short and long-term aged asphalt mixtures for low-temperature performance." *Constr. Build. Mater.* 319 (Feb): 126038. https://doi.org/10.1016/j.conbuildmat.2021.126038.

Casado-Barrasa, R., P. Lastra-Gonzalez, I. Indacoechea-Vega, and D. Castro-Fresno. 2019. "Assessment of carbon black modified binder in a sustainable asphalt concrete mixture." *Constr. Build. Mater.* 211 (Jun): 363–370. https://doi.org/10.1016/j.conbuildmat.2019.03.255.

Chen, A., Q. Deng, Y. Li, Z. Chen, J. Li, J. Feng, F. Wu, S. Wu, Q. Liu, and C. Li. 2022. "Harmless treatment and environmentally friendly application of waste tires—TPCB/TPO composite-modified bitumen." *Constr. Build. Mater.* 325 (Mar): 126785. https://doi.org/10.1016/j.conbuildmat.2022.126785.

Cui, P. D., S. P. Wu, Y. Xiao, R. Hu, and T. Y. Yang. 2021. "Environmental performance and functional analysis of chip seals with recycled basic oxygen furnace slag as aggregate." *J. Hazard. Mater.* 405 (Mar): 124441. https://doi.org/10.1016/j.jhazmat.2020.124441.

Duarte, G. M., and A. L. Faxina. 2021. "Asphalt concrete mixtures modified with polymeric waste by the wet and dry processes: A literature review." *Constr. Build. Mater.* 312 (Dec): 125408. https://doi.org/10.1016/j.conbuildmat.2021.125408.

Feng, Z., P. Zhao, X. Li, and L. Zhu. 2021. "Preparation and properties of bitumen modified with waste rubber pyrolytic carbon black." *Constr. Build. Mater.* 282 (May): 122697. https://doi.org/10.1016/j.conbuildmat.2021.122697.

Geckil, T., P. Ahmedzade, and T. Alatas. 2018. "Effect of carbon black on the high and low temperature properties of bitumen." *Int. J. Civ. Eng.* 16 (2a): 207–218. https://doi.org/10.1007/s40999-016-0120-4.

Guo, J. L., Y. P. Bao, and M. Wang. 2018. "Steel slag in China: Treatment, recycling, and management." *Waste Manage.* 78 (Aug): 318–330. https://doi.org/10.1016/j.wasman.2018.04.045.

Huang, J. D., G. S. Kumar, and Y. T. Sun. 2021. "Evaluation of workability and mechanical properties of asphalt binder and mixture modified with waste toner." *Constr. Build. Mater.* 276 (Mar): 122230. https://doi.org/10.1016/j.conbuildmat.2020.122230.

Jahanbakhsh, H., M. M. Karimi, B. Jahangiri, and F. Moghadas Nejad. 2018. "Induction heating and healing of carbon black modified asphalt concrete under microwave radiation." *Constr. Build. Mater.* 174 (Jun): 656–666. https://doi.org/10.1016/j.conbuildmat.2018.04.002.

Konell, J. P. 2002. "Characterization and tensile modulus modeling of conductive resins." Doctoral thesis, Michigan Technological Univ. https://www.proquest.com/openview/2c6cd36a53372f2b848803c3c528141f/1?pq-origsite=gscholar&cbl=18750&diss=y.

Korayem, A. H., H. Ziari, M. Hajiloo, M. Abarghooie, and P. Karimi. 2020. "Laboratory evaluation of stone mastic asphalt containing amorphous carbon powder as filler material." *Constr. Build. Mater.* 243 (May): 118280. https://doi.org/10.1016/j.conbuildmat.2020.118280.

Kumar, A., R. Choudhary, and A. Kumar. 2022. "Performance evaluation of asphalt binders modified with pyrolytic chars and WMA additive." *Mater. Today: Proc.* 65 (Jan): 1823–1830. https://doi.org/10.1016/j.matpr.2022.04.969.

La Rosa, A. D., E. Pergolizzi, D. Maragna, G. Recca, and G. Cicala. 2019. "Reuse of carbon black from end-of-life tires in new pneumatic formulations and life-cycle assessment of the thermolysis process." *J. Elastomers Plast.* 51 (7–8): 740–754. https://doi.org/10.1177/0095244318819242.

Lastra-Gonzalez, P., J. Rodriguez-Hernandez, C. Real-Gutierrez, D. Castro-Fresno, and A. Vega-Zamanillo. 2022. "Effect of different types of 'dry way' additions in porous asphalt mixtures." *Materials* 15 (4): 1549. https://doi.org/10.3390/ma15041549.

Lee, K., and S. Kim. 2022. "Performance improvement effect of asphalt binder using pyrolysis carbon black." *Materials* 15 (12): 4158. https://doi.org/10.3390/ma15124158.

Lee, K.-H. 2016. "Performance evaluation of dense graded asphalt mixture modified by pyrolysis carbon black." *J. Korea Acad. Ind. Cooperation Soc.* 17 (3): 732–737. https://doi.org/10.5762/KAIS.2016.17.3.732.

Li, H., Z. Feng, H. Liu, A. T. Ahmed, M. Zhang, G. Zhao, P. Guo, and Y. Sheng. 2022a. "Performance and inorganic fume emission reduction of desulfurized rubber powder/styrene–butadiene–styrene composite modified asphalt and its mixture." *J. Cleaner Prod.* 364 (Sep): 132690. https://doi.org/10.1016/j.jclepro.2022.132690.

Li, N., Q. Jiang, F. S. Wang, P. D. Cui, J. Xie, J. S. Li, S. P. Wu, and D. M. Barbieri. 2021a. "Comparative assessment of asphalt volatile organic compounds emission from field to laboratory." *J. Cleaner Prod.* 278 (Jan): 123479. https://doi.org/10.1016/j.jclepro.2020.123479.

Li, R., Z. Leng, J. Yang, G. Y. Lu, M. Huang, J. T. Lan, H. L. Zhang, Y. W. Bai, and Z. J. Dong. 2021b. "Innovative application of waste polyethylene terephthalate (PET) derived additive as an antistripping agent for asphalt mixture: Experimental investigation and molecular dynamics simulation." *Fuel* 300 (Sep): 121015. https://doi.org/10.1016/j.fuel.2021.121015.

Li, Y., J. Li, C. Li, A. Chen, T. Bai, S. Tang, S. Wu, Y. Gao, H. Zhu, and J. Feng. 2022b. "Strength formation mechanism and performance of steel slag self-compacting epoxy resin concrete." *Constr. Build. Mater.* 359 (Dec): 129525. https://doi.org/10.1016/j.conbuildmat.2022.129525.

Liu, J. W., P. W. Hao, Z. S. Dou, J. B. Wang, and L. J. Ma. 2021. "Rheological, healing and microstructural properties of unmodified and crumb rubber modified asphalt incorporated with graphene/carbon black composite." *Constr. Build. Mater.* 305 (Oct): 124512. https://doi.org/10.1016/j.conbuildmat.2021.124512.

Liu, X., X. L. Zou, X. L. Yang, and Z. W. Zhang. 2018. "Effect of material composition on antistripping performance of SBS modified asphalt mixture under dry and wet conditions." *J. Adhes. Sci. Technol.* 32 (14): 1503–1516. https://doi.org/10.1080/01694243.2018.1426973.

Lu, G., P. Liu, T. Torzs, D. Wang, M. Oeser, and J. Grabe. 2020a. "Numerical analysis for the influence of saturation on the base course of permeable pavement with a novel polyurethane binder." *Constr. Build. Mater.* 240 (Apr): 117930. https://doi.org/10.1016/j.conbuildmat.2019.117930.

Lu, G., Z. Wang, P. Liu, D. Wang, and M. Oeser. 2020b. "Investigation of the hydraulic properties of pervious pavement mixtures: Characterization of Darcy and non-Darcy flow based on pore microstructures." *J. Transp. Eng. Part B. Pavements* 146 (2): 04020012. https://doi.org/10.1061/JPEODX.0000161.

Luo, H. S., C. F. Zheng, B. X. Liu, C. H. Bao, B. W. Tian, and W. Y. Liu. 2022a. "Study on SBS modifier of bio-oil/sulfur compound under dry modification mode." *Constr. Build. Mater.* 326 (Apr): 127059. https://doi.org/10.1016/j.conbuildmat.2022.127059.

Luo, H. S., C. F. Zheng, X. Yang, C. H. Bao, W. Y. Liu, and Z. Lin. 2022b. "Development of technology to accelerate SBS-modified asphalts swelling in dry modification mode." *Constr. Build. Mater.* 314 (Jan): 125703. https://doi.org/10.1016/j.conbuildmat.2021.125703.

Min, K. E., and H. M. Jeong. 2013. "Characterization of air-blown asphalt/trans-polyoctenamer rubber blends." *J. Ind. Eng. Chem.* 19 (2): 645–649. https://doi.org/10.1016/j.jiec.2012.09.017.

MOT (Ministry of Transport of the People's Republic of China). 2005. *Test methods of aggregate for highway engineering*. JTG E42-2005. Beijing: MOT.

MOT (Ministry of Transport of the People's Republic of China). 2011. *Standard test methods of bitumen and bituminous mixtures for highway engineering*. JTG E20. Beijing: MOT.

Negulescu, I., L. Mohammad, W. Daly, C. Abadie, R. Cueto, C. Daranga, and I. Glover. 2006. "Chemical and rheological characterization of wet and dry aging of SBS copolymer modified asphalt cements: Laboratory and field evaluation (with discussion)." In Vol. 75 of *Association of asphalt paving technologists*. Baton Rouge, LA: Louisiana State University.

Park, T., and C. Lovell. 1996. *Using pyrolized carbon black (PCB) from waste tires in asphalt pavement (part 1, limestone aggregate)*. FHWA/IN/JHRP-95/10. West Lafayette, IN: Purdue Univ.

Parthasarathy, P., H. S. Choi, H. C. Park, J. G. Hwang, H. S. Yoo, B. K. Lee, and M. Upadhyay. 2016. "Influence of process conditions on product yield of waste tyre pyrolysis—A review." *Korean J. Chem. Eng.* 33 (8): 2268–2286. https://doi.org/10.1007/s11814-016-0126-2.

Przydatek, G., G. Budzik, and M. Janik. 2022. "Effectiveness of selected issues related to used tyre management in Poland." *Environ. Sci. Pollut. Res.* 29 (21): 31467–31475. https://doi.org/10.1007/s11356-022-18494-7.

Sugatri, R. I., Y. C. Wirasadewa, K. E. Saputro, E. Y. Muslih, R. Ikono, and M. Nasir. 2018. "Recycled carbon black from waste of tire industry: Thermal study." *Microsyst. Technol.* 24 (1): 749–755. https://doi.org/10.1007/s00542-017-3397-6.

Sun, X. L., X. Qin, Z. S. Liu, Y. M. Yin, S. Jiang, and X. C. Wang. 2020. "Applying feasibility analysis and catalytic purifying potential of novel modifying agent used in asphalt pavement materials." *Constr. Build. Mater.* 245 (Jun): 118467. https://doi.org/10.1016/j.conbuildmat.2020.118467.

Wang, F., et al. 2022. "Microwave heating mechanism and self-healing performance of scrap tire pyrolysis carbon black modified bitumen." *Constr. Build. Mater.* 341 (Jul): 127873. https://doi.org/10.1016/j.conbuildmat.2022.127873.

Wang, F. S., J. Xie, S. P. Wu, J. S. Li, D. M. Barbieri, and L. Zhang. 2021. "Life cycle energy consumption by roads and associated interpretative analysis of sustainable policies." *Renewable Sustainable Energy Rev.* 141 (May): 110823. https://doi.org/10.1016/j.rser.2021.110823.

Wu, H., L. Wang, J. Hu, and X. Luo. 2022. "Evaluation of low-temperature performance of SBS/CR composite modified-asphalt mixture under aging and freeze thaw cycles." *J. Mater. Civ. Eng.* 34 (10): 04022239. https://doi.org/10.1061/(ASCE)MT.1943-5533.0004395.

Wu, X. W., D. W. Cao, and H. Y. Zhang. 2011. "Influence of carbon black on storage stability of HDPE-SBS modified asphalt." *Adv. Mater. Res.* 374–377 (Jan): 1409–1413. https://doi.org/10.4028/www.scientific.net/AMR.374-377.1409.

Xu, J., J. Yu, W. He, J. Huang, J. Xu, and G. Li. 2021. "Wet compounding with pyrolytic carbon black from waste tyre for manufacture of new tyre—A mini review." *Waste Manage Res.* 39 (12): 1440–1450. https://doi.org/10.1177/0734242X211004746.

Yang, X., G. Liu, H. Rong, Y. Meng, C. Peng, M. Pan, Z. Ning, and G. Wang. 2022. "Investigation on mechanism and rheological properties of bio-asphalt/PPA/SBS modified asphalt." *Constr. Build. Mater.* 347 (Sep): 128599. https://doi.org/10.1016/j.conbuildmat.2022.128599.

Zhang, P., L. Ouyang, L. Yang, Y. Yang, G. F. Lu, and T. Huang. 2021. "Laboratory investigation of carbon black/bio-oil composite modified asphalt." *Materials* 14 (17): 4910. https://doi.org/10.3390/ma14174910.

Zhang, S. L., Z. X. A. Xin, Z. X. Zhang, and J. K. Kim. 2009. "Characterization of the properties of thermoplastic elastomers containing waste rubber tire powder." *Waste Manage.* 29 (5): 1480–1485. https://doi.org/10.1016/j.wasman.2008.10.004.